

4.2.10 Mogoin Gol 2

A schematic summary of the geology for the prospect area is shown in Figure 4.26, while examples of data are shown in Figure 4.27. This area consists predominantly of two late Permian volcano-sedimentary sequences and a series of igneous intrusive units. The Permian sediments have a distinctive relative low, flat magnetic response, while the volcanic units have a moderate to high response with sub-linear character. There is a weak E - W trend shown by the long elliptical axes of zoned intrusive bodies and the strike of linear volcanic units.

A number of the intrusive units appear to be truncated to the S (407967mE 5461075mN and 410972mE 5457300mN). This may indicate that either E - W or ENE - WSW trending faults (or thrusts) are present within this area, although the contrast in the magnetic data is too slight to be certain.

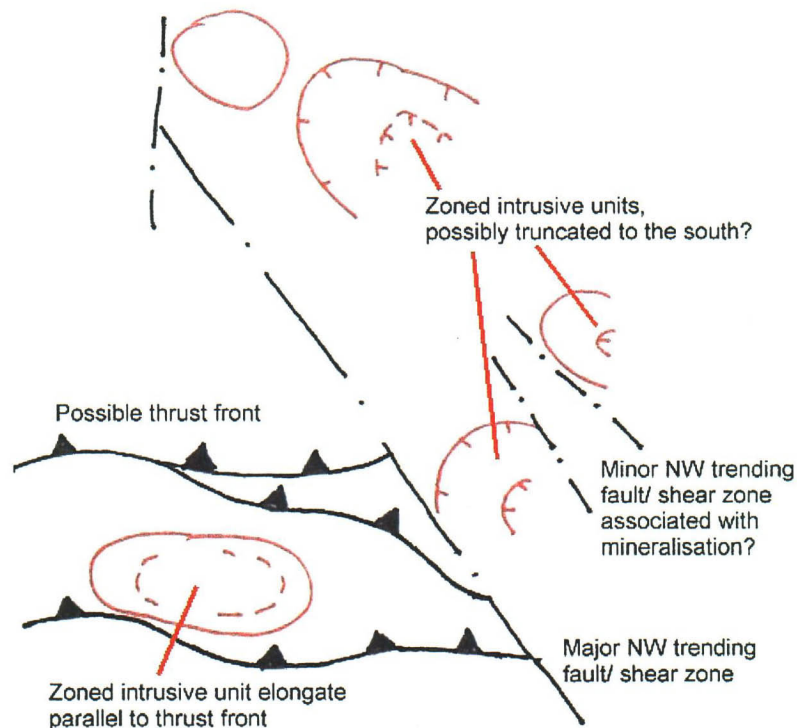
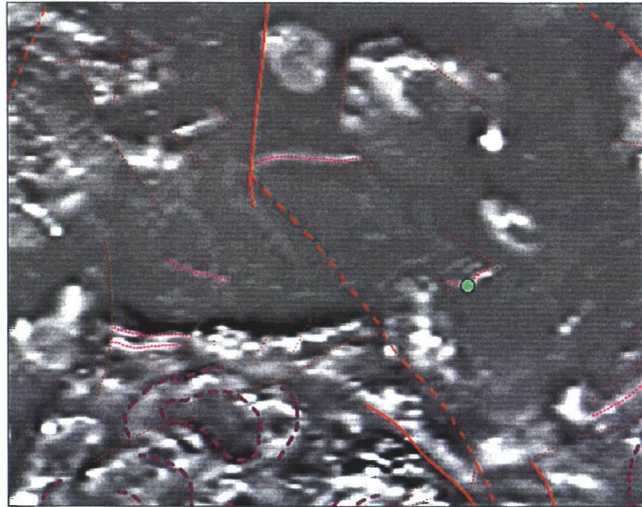
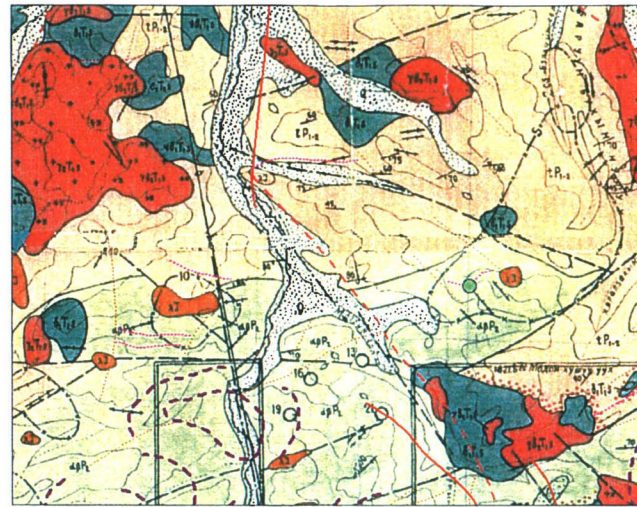


Figure 4.26: Schematic representation of possible thrusts and truncation of igneous bodies.

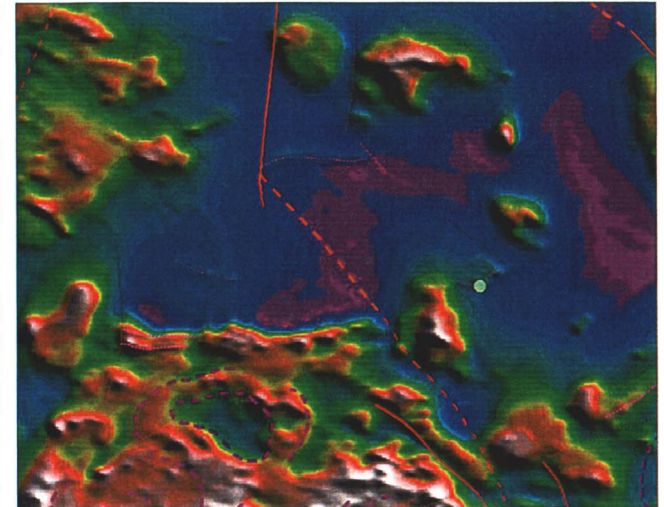
Radiometric data appears to have a partially similar distribution to the published mapping although there is potential to improve the interpretation. Main areas of high K coincide with mapped granitic units.



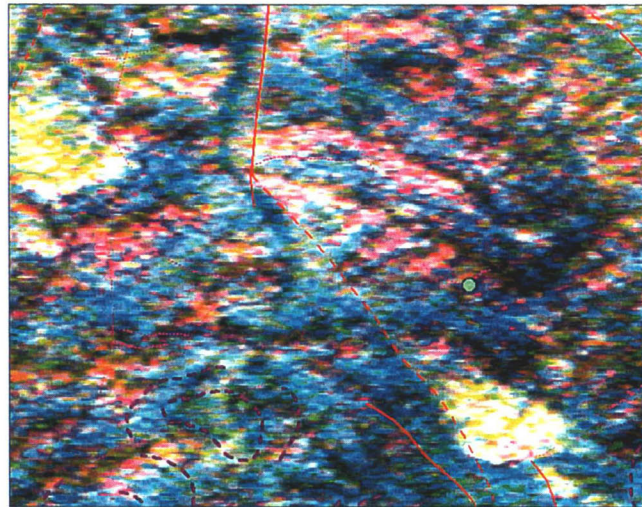
A



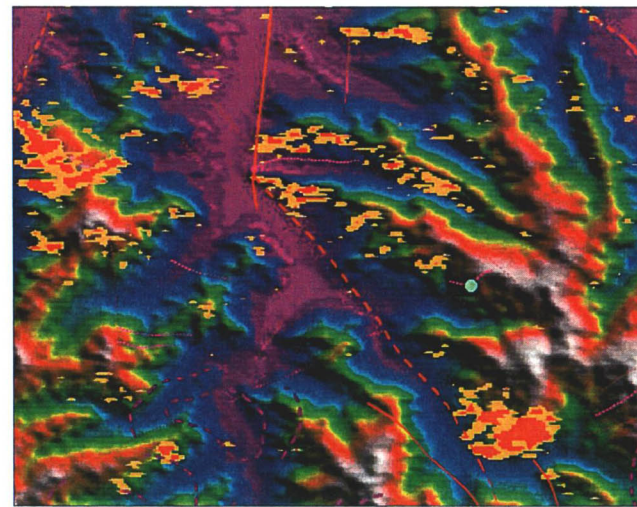
B



C



D



E



F

A-273

Figure 4.27: Characteristics of the Mogoin Gol 2 area.

4.2.11 Meij Uul

Examples of data for the prospect area are shown in Figure 4.31. This area consists predominantly of Triassic to Jurassic volcano-sedimentary units. These typically have a moderate to high relative magnetic intensity, short wavelength response. The dominant structures in the area consist of a broad zone (up to 4 km wide) of NW trending shear zones. These structures could possibly have a right lateral strike-slip displacement and a 'late' normal displacement with downthrow to the NE and are interpreted to be the main structures that divide domain 3 from domain 4.

Known areas of mineralisation appear to be associated with approximately N – S trending structures. These N – S trending faults may be 'late' extensional structures associated with the shear zones, however, there is little information to further constrain these mineralised areas.

Radiometric data appears to provide a slightly different distribution of surface material to that proposed from the published mapping. Detailed analysis of the data may enable a more accurate litho-magnetic interpretation to be made. There appears to be minimal direct evidence for potassic alteration in this area.

A-277

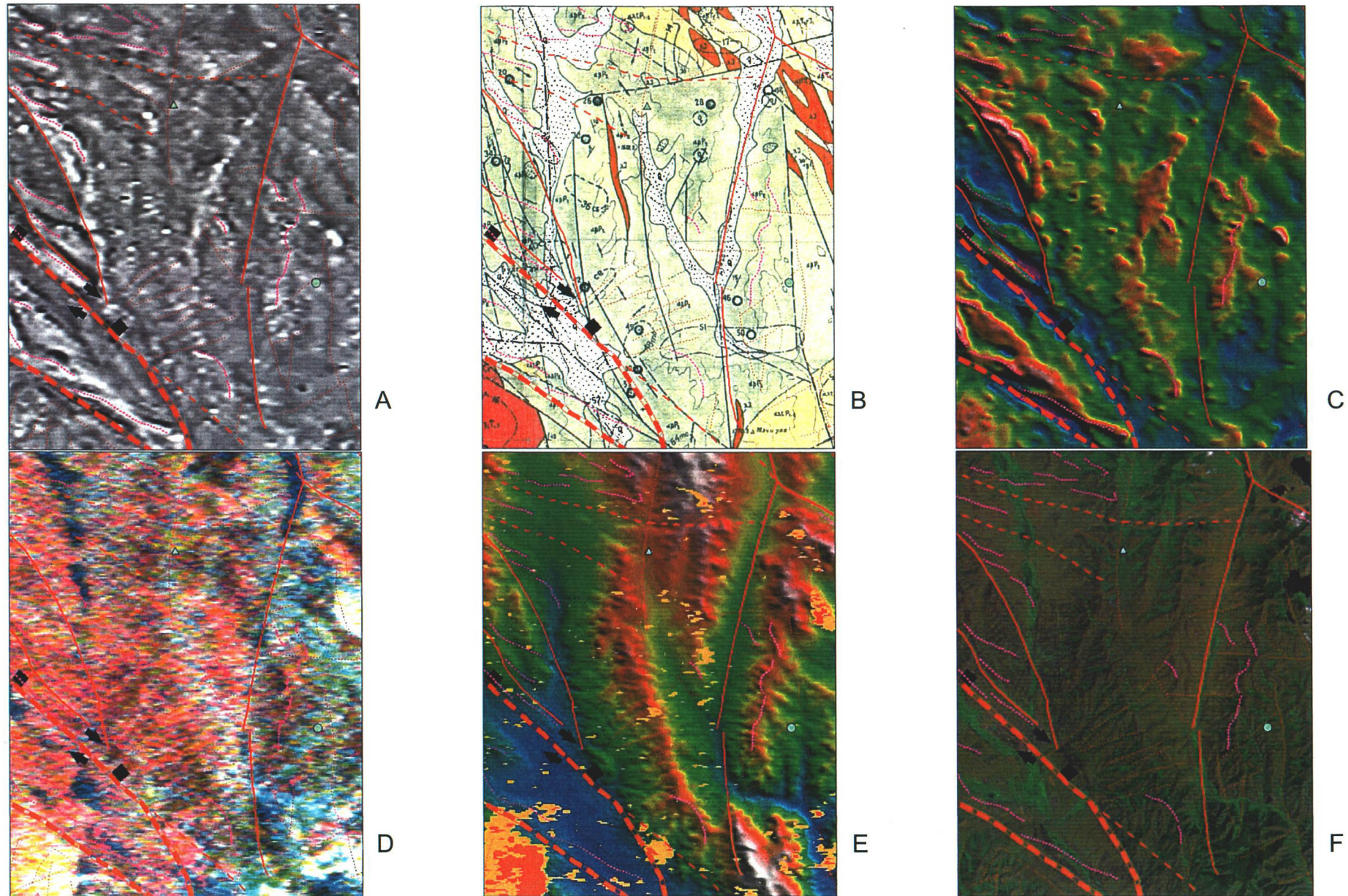


Figure 4.28: Characteristics of the Mej Uul area.

4.2.12 Undrakh

A schematic summary of the geology for the prospect area is shown in Figure 4.29, while examples of data are shown in Figure 4.30. The main feature of this area is the large, zoned igneous unit, with its elongate N - S trending ellipsoidal axis. This igneous body is subdivided by an approximate NW to NNW trending fault with a left lateral displacement (355150mE 5399500mN). It is also bound to the SW by a similar trending structure (334000mE 5396000mN). Minor faults with varying strike occur around the intrusive body and are probably radial fractures associated with intrusion.

A distinctive anomalous NW to NNW trending zone with a relative low magnetic intensity occurs about 334600mE 5394900mN. This area may represent a 'late' intrusive unit with a different magnetic polarity to the surrounding igneous host, or may represent an intensely altered area.

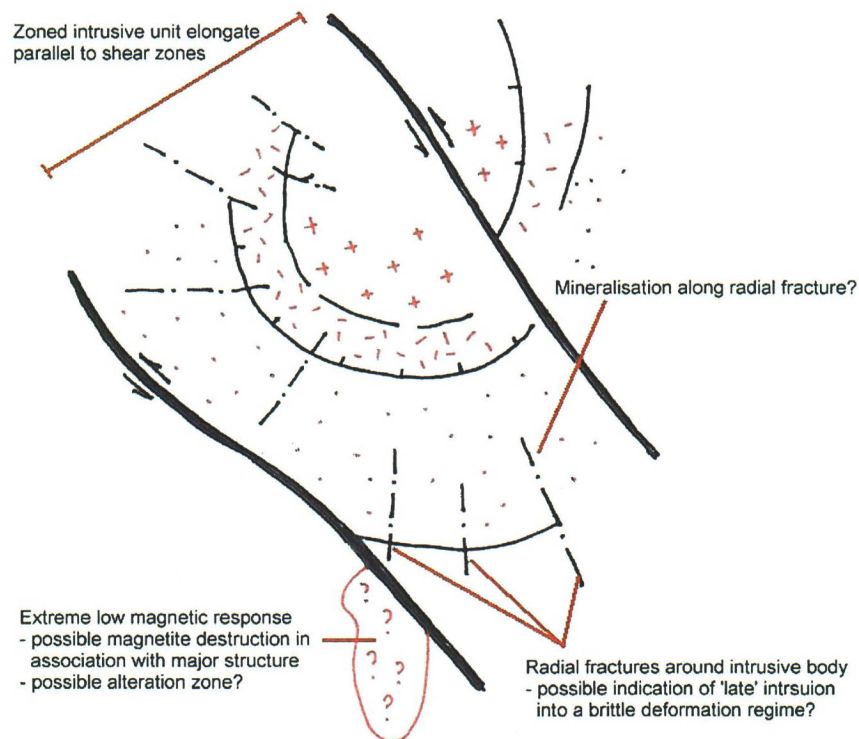
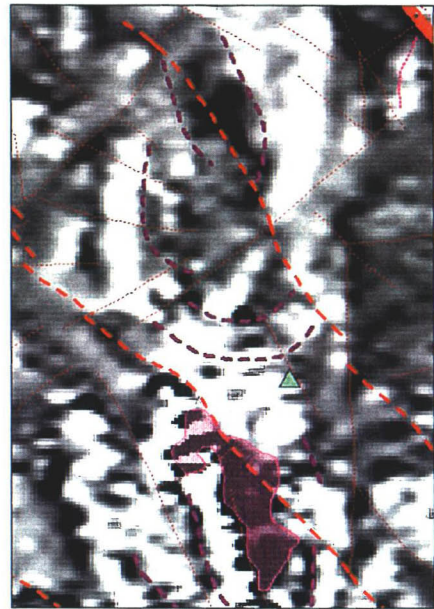
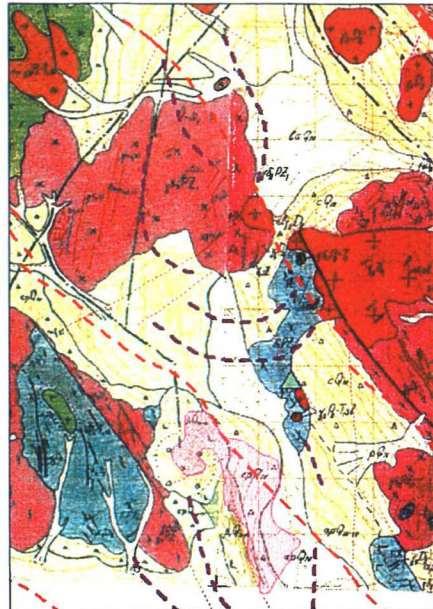


Figure 4.29: Schematic representation of radial fracturing around an intrusive body.

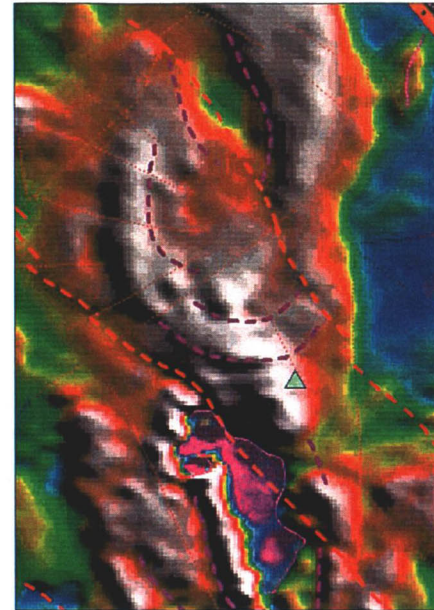
Radiometric data appears to provide a different distribution of surface material to that proposed from the published mapping. Detailed analysis of the data may enable a more accurate litho-magnetic interpretation to be made.



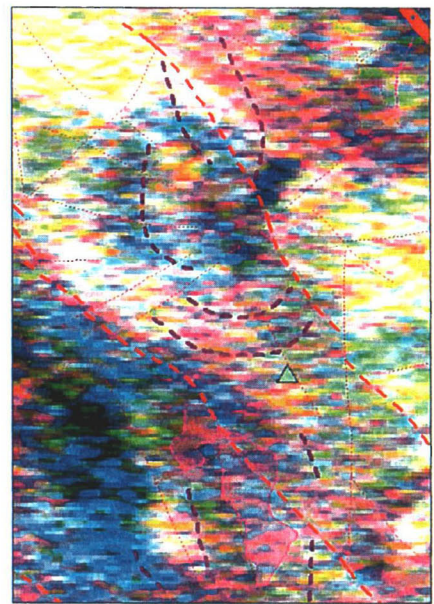
A



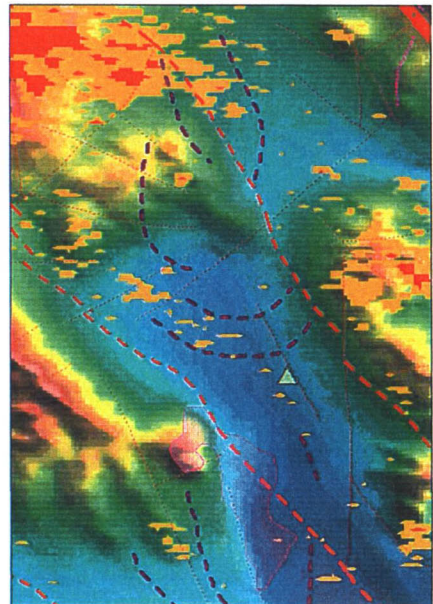
B



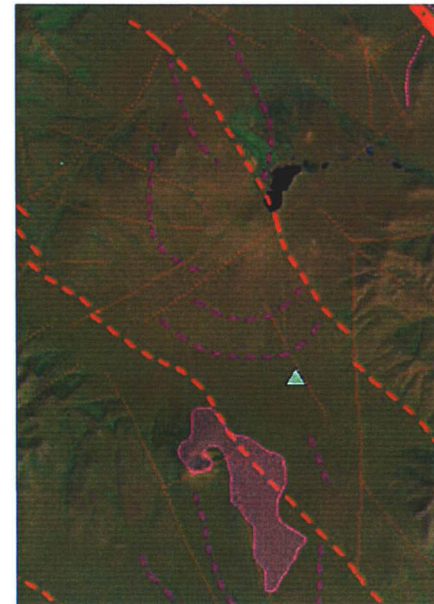
C



D



E



F

Figure 4.30: Characteristics of the Undrakh area.

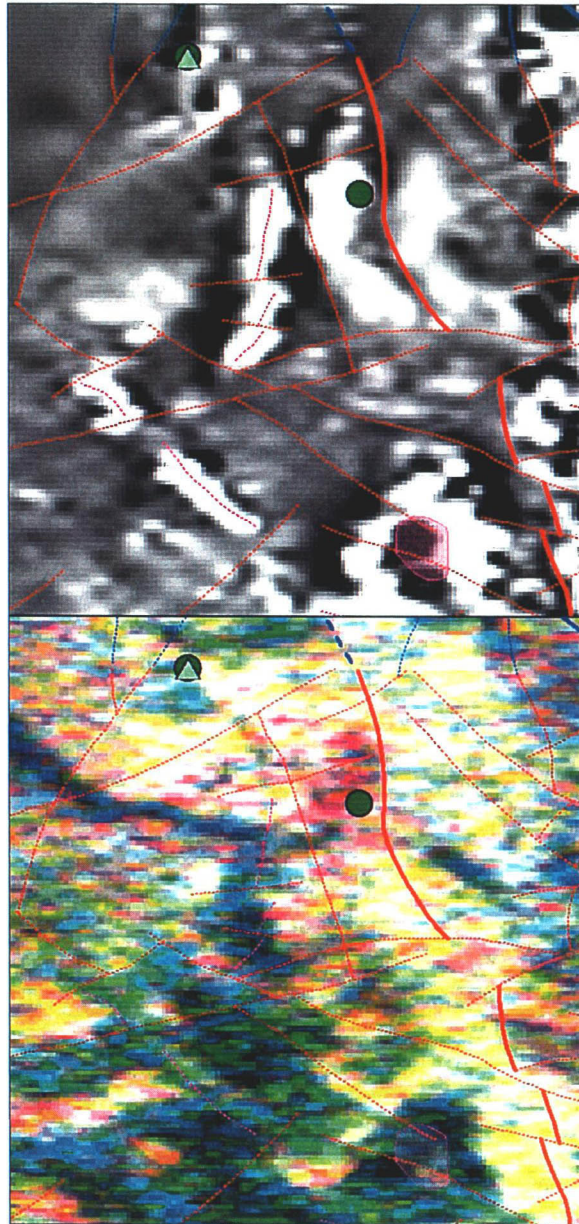
4.2.13 Umin Tsagaan Nuu

Examples of data for the prospect area are shown in Figure 4.28. The area appears to consist of sedimentary units underlain and intruded by a complex mixture of igneous units. There is little to no apparent correlation of the distribution of magnetic units with the mapped surface geology and the area may benefit from a litho-magnetic interpretation. The area is extensively fractured and faulted, with the dominant strike approximately N - S. Apart from the close proximity to faults and the high K potassium response there is little information to further constrain the cause of mineralisation in this area.

Radiometric data appears to provide a different distribution of surface material to that proposed from the published mapping. Drainage provides a distinctive low response. Detailed analysis of the data may enable a more accurate litho-magnetic interpretation to be made.

Potassium enrichment is present between the main areas of mineralisation at Umin Tsagaan Nuu (347000mE 5407300mN) and Aguit (349400mE 5405400mN) as shown by the clipped 95 and 99% clipped data. The high K values may have a slight NNE elongate trend that may indicate an association with faults. However, a high response is also noted trending NNW that probably relates to locally derived colluvium and field verification is required to determine the significance of the radiometric response in this area. Of significance is that a high Potassium response (red) is noted around the Aguit mineralisation, but lost when the data is clipped. This emphasises the caution required to assess the radiometric data.

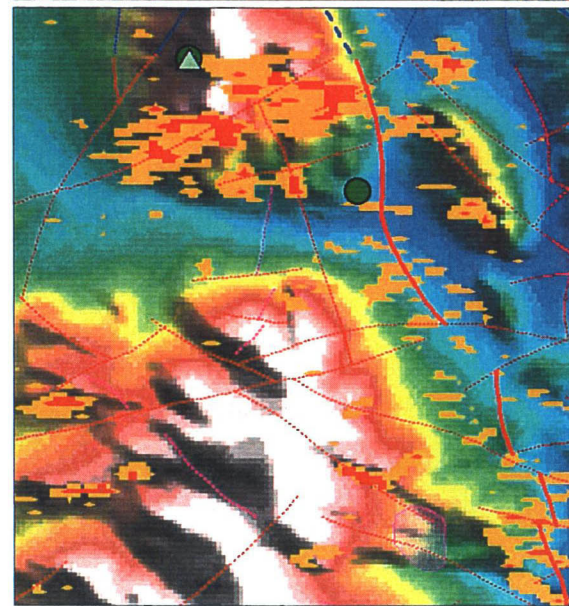
A-285



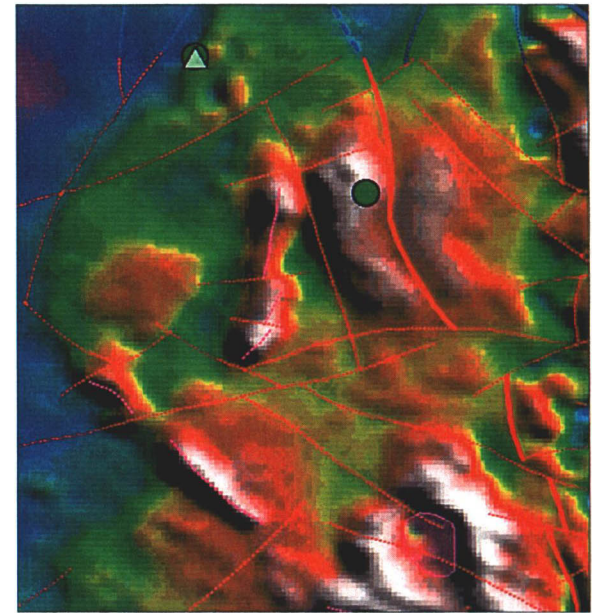
A



B



D



C



F

Figure 4.31: Characteristics of the Umin Tsagaan Nuu area.

4.2.14 Tsookhor Morit

A schematic summary of the geology for the prospect area is shown in Figure 4.32, while examples of data are shown in Figure 4.33. The area appears to consist of at least two major lithological units (with a shallow magnetic source) separated by a well-defined, arcuate fault zone, convex to the S. This fault zone has a relative low magnetic intensity and may be associated with magnetite destruction. Numerous 'late' minor faults, perpendicular to and radially distributed along the main fault zone, trend NE - SW to N - S and cross-cut and offset the main arcuate faults. A concentration of NE trending faults to the E of Tsookhor Morit may act as a major fluid pathway creating an increase in the magnetite destruction along a broad corridor.

A possible explanation for the arcuate and radial fault patterns may be that they represent a ring fracture (caldera) and associated radial fractures. This would require an intrusive body to be present at depth to the NE, with the survey only covering the bottom SW quadrant.

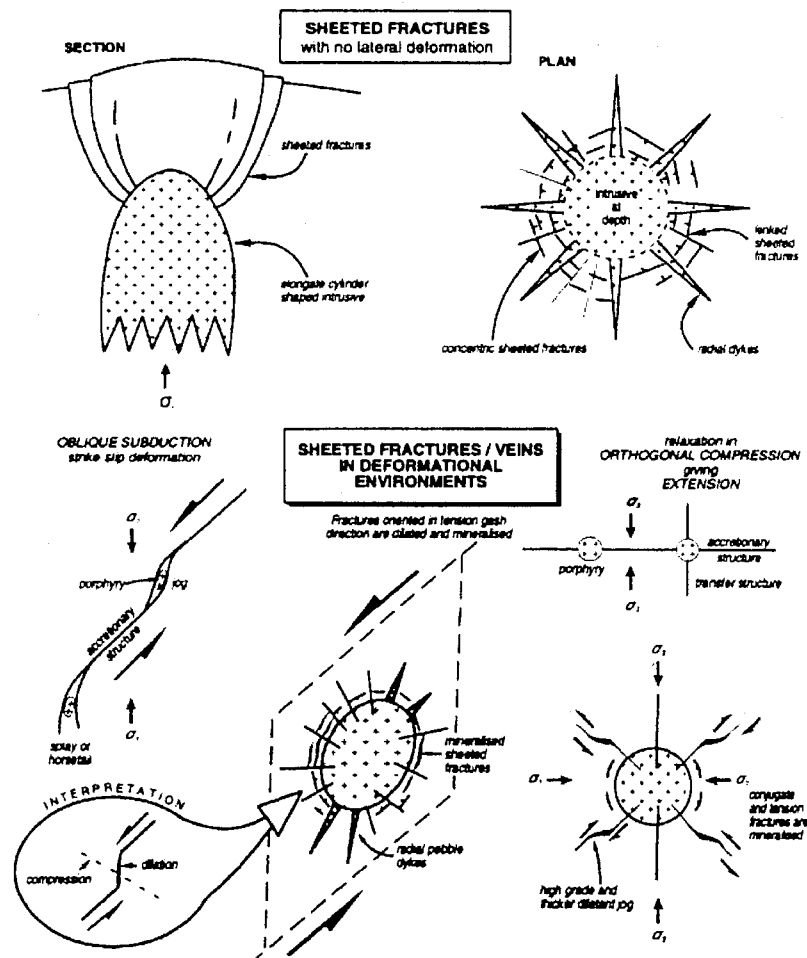


Figure 4.32: Schematic representation of radial fracturing around a possible intrusive body (from Corbett and Leach 1995).

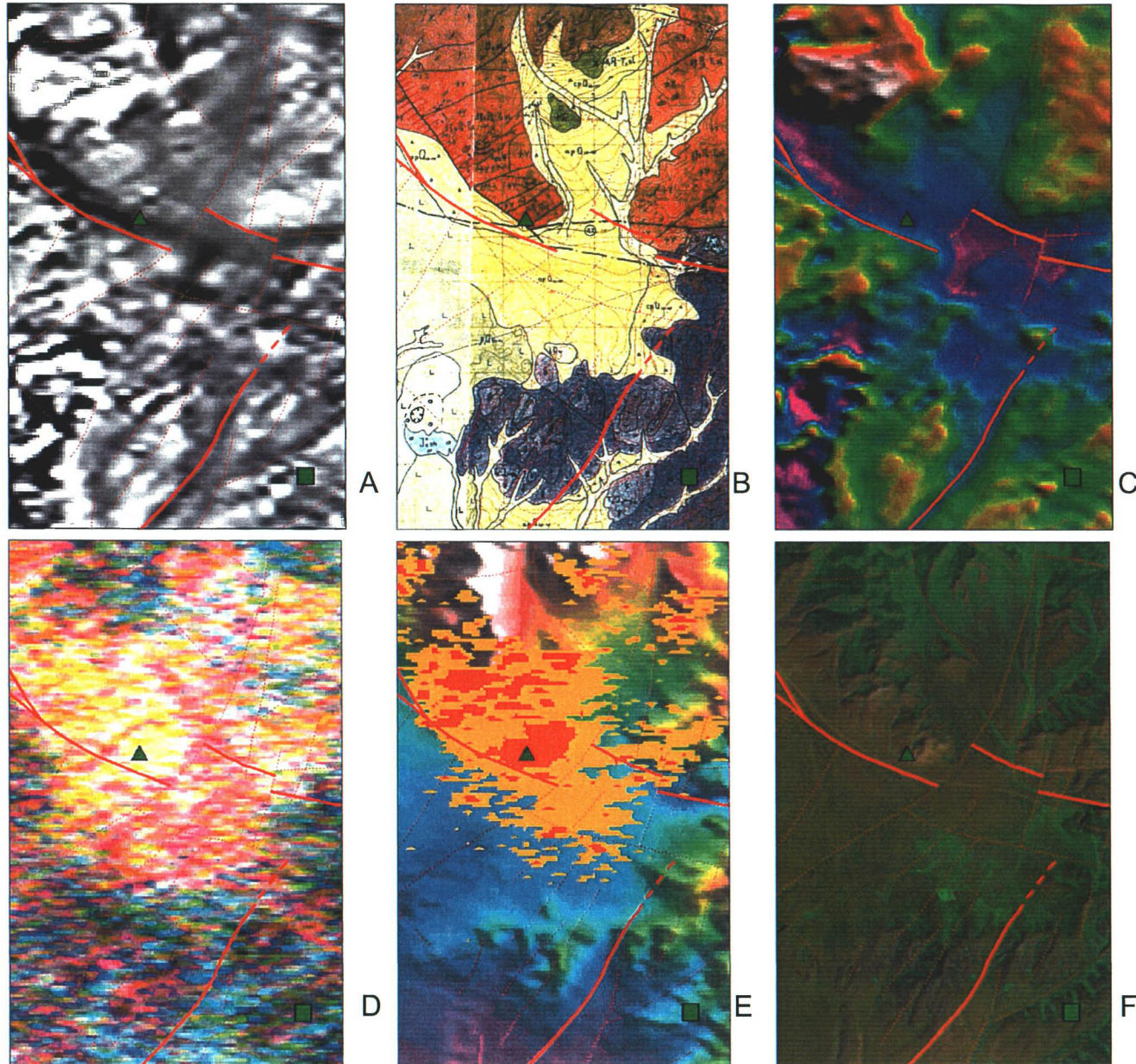


Figure 4.33: Characteristics of the Tsookhor Morit prospect area.

Radiometric data appears to provide a different distribution of surface material to that proposed from the published mapping. Detailed analysis of the data may enable a more accurate litho-magnetic interpretation to be made. A large K enrichment zone is present around the main area of mineralisation at Tsookhor Morit (372500mE 5401000mN). The highest values (99% clip, shown in red) also have a slight NE elongate trend that may indicate an association with faults. The magnetic data also supports the probability of NE trending structures in this area. However, the high response may be due to the host lithology and locally derived colluvial material and field verification is required. A slight K enrichment response occurs around the mineralised area at Khar Uul (376100mE 5395500mN). Although not as spectacular an anomaly as at Tsookhor Morit, it is potentially just as significant with the difference between the two areas most likely due to the host lithology.